

Electrical characteristics of epitaxial MCT after As⁺ implantation

This content has been downloaded from IOPscience. Please scroll down to see the full text.

2017 J. Phys.: Conf. Ser. 830 012083

(<http://iopscience.iop.org/1742-6596/830/1/012083>)

View [the table of contents for this issue](#), or go to the [journal homepage](#) for more

Download details:

IP Address: 188.162.84.48

This content was downloaded on 10/05/2017 at 06:40

Please note that [terms and conditions apply](#).

You may also be interested in:

[Electrical activation of arsenic implanted in SOI](#)

R M de Oliveira, M Dalponte and H Boudinov

[Combined frequency- and time-domain photocarrier radiometry characterization of ion-implanted and thermally annealed silicon wafers](#)

Ren Sheng-Dong, Li Bin-Cheng, Gao Li-Feng et al.

Electrical characteristics of epitaxial MCT after As⁺ implantation

A Voitsekhovskii¹, I Izhnin^{1,3}, A Korotaev¹, D Lyapunov¹, S Dvoretiskii²,
P Smirnov²

¹National Research Tomsk State University, Tomsk, 634050, Russia

²A.V. Rzhzanov Institute of Semiconductor Physics, Siberian Branch of the Russian Academy of Sciences, Novosibirsk, 630090, Russia

³R&D Institute for Materials SRC "Carat", Lviv, 79031, Ukraine

E-mail: dima.lyapunov_1992@mail.ru

Abstract. In this work we studied the characteristics of MBE MCT films after the introduction of different energies As⁺ with different doses of irradiation. Some of the samples were subjected to post-implantation annealing. Electrical characteristics of the samples were determined from Hall measurements. Voltage-current characteristics of the structures were also measured. Activation As and modification of the characteristics of MCT outside the implanted layer after annealing have been detected. Also we found differences in the p-n junction depths and electrically active defects profiles.

1. Introduction

At present molecular beam epitaxial (MBE) layers of mercury-cadmium-telluride HgCdTe (MCT) solid solutions are widely used to create multi-element semiconductor detectors of IR radiation providing signal processing directly in the focal region [1]. Along with the study of the initial properties of epitaxial films of MCT grown by MBE, forming a p-n junction by ion implantation is an urgent problem.

For various reasons (in particular, to reduce the dark currents) there appears more advantageous manufacturing photodiode structure of "p-on-n" type. In [2] it was shown that in such structure dark currents become smaller by two orders of magnitude. This is due to low mobility and lifetime of holes that there are minority carriers for the n-base of a photodiode. Reducing dark current increases the photosensitivity of such a structure. But for such structures smaller yields of detectors (5% less) and a higher level of inhomogeneities per unit of area of photodiode array are typical. This is due, primarily, to the lack of understanding of mechanisms of radiation defect formation and the formation of a p-n junction in such structures. These mechanisms underlie the processes of manufacturing "p-on-n" structures.

The aim of this work was to study the characteristics of MBE MCT films, after the introduction of different energies As⁺ with different doses of irradiation.

2. Samples and measurement procedure

The epitaxial films were grown at the Semiconductor Physics Institute of the Siberian Branch of the Russian Academy of Sciences. After growth, the films had n-type conductivity, for conversion to p-



type conductivity, the films were annealed in a neutral atmosphere of hydrogen or helium. The parameters of the samples are given in Table 1.

Arsenic ion implantation was carried out at the Institute of Semiconductor Physics in Novosibirsk on the plant ion implantation. Irradiation of arsenic ions was performed at room temperature in a dosage range 10^{13} - 10^{15} cm^{-2} . The parameters of the ion beam are as follows: energy ions $E_1 = 190$ keV (samples 1-5 series), $E_2 = 350$ keV for sample 5 series). The ion current density is $j = 0.06$ $\mu\text{A}\times\text{cm}^{-2}$. As shown in ref. [2], for these ion currents we can neglect heating of the sample during the implantation process. After the implantation for the fifth series of samples of the two-stage activation annealing was conducted.

Table 1. Parameters of the samples.

series	d, μm	p, cm^{-3}	μ_p , $\text{cm}^2\text{V}^{-1}\text{s}^{-1}$
1	7.56	$1.5 \cdot 10^{16}$	334.444
2	7.06	$2.7 \cdot 10^{16}$	200.116
3	15.51	$1.2 \cdot 10^{16}$	428.118
4	14.7	$1.57 \cdot 10^{16}$	462.414
5 (n-type)	7.41	$7.4 \cdot 10^{14}$	9500

Measurements of the electrophysical parameters of the samples were made at the temperature of liquid nitrogen using the Hall method in the Van-der-Pau configuration. The electron concentration distribution as a function of semiconductor depth was determined by the method of differential Hall measurements using an etching process. The error in the Hall and conductivity measurements did not exceed 2-3%. The error in the volume concentration and mobility of charge carrier measurements is mainly determined by the accuracy in the measurement of the thickness of the removed layer and did not exceed 10-12%.

To determine the depth of the p-n transition 3 samples were selected which produced mesa structure. The height of the mesa was changed with the step of 1 micron by chemical etching. Measurements of current-voltage characteristics of the samples were performed using the automated spectroscopy admittance nanoheterostructures equipment. It permits quantitative measurements of electrical parameters of materials and nanostructures and microelectronics.

3. Experimental results and discussion

Measurement of the electro-physical parameters of the samples after implantation shows that As ion irradiation resulted in a conversion of the conduction type, with the formation of a highly alloyed n^+ -layer in the surface of the material due to the generation of radiation defects, which is characteristic of MCT. The dependence of the layer charge carrier concentration N_S on the radiation dose Φ is shown in Figure 1.

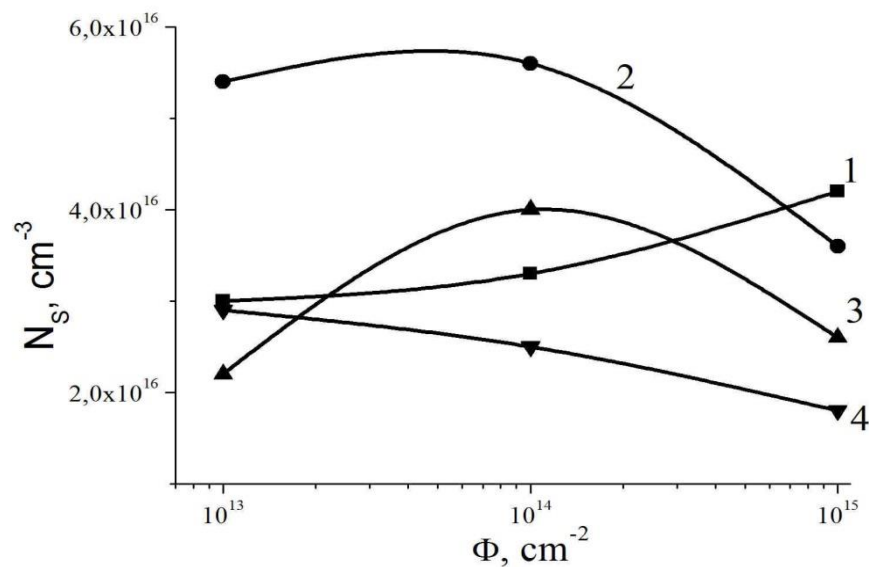


Figure 1. The dependence of the electron concentration N_S on the radiation dose. Curves numbers correspond to the samples of series.

The figure shows that the concentration decrease is observed at higher doses of radiation, which is contrary to the argon implantation data [3]. This decline can be attributed to the greater disorder of the implanted layer by applying a high-energy and heavier (by 1.9 times in comparison with argon ions) arsenic ions.

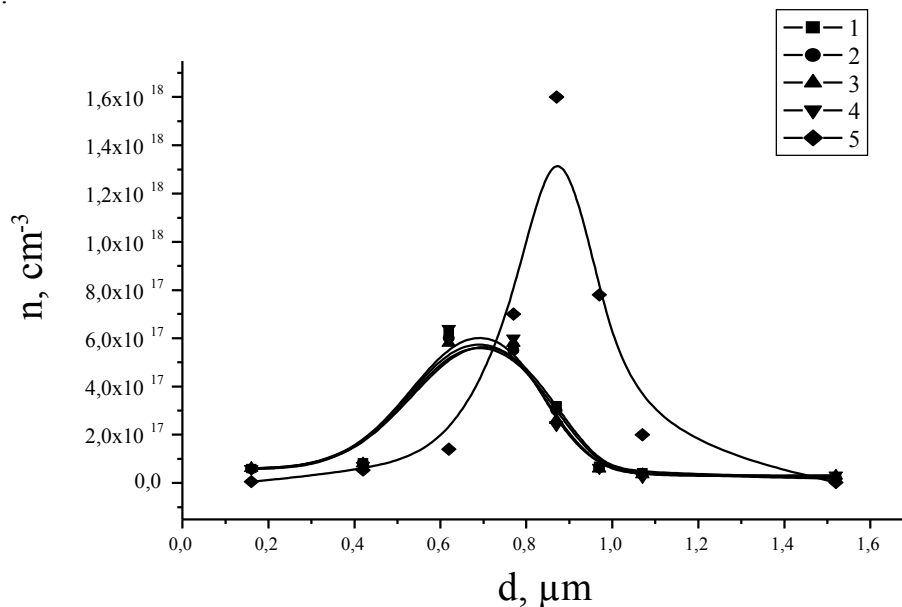


Figure 2. The dependence of the electron concentration n on the depth. Curves numbers correspond to the samples of series. $\Phi = 10^{14} \text{ cm}^{-2}$.

The profiles of the carrier concentration are shown in Figure 2. It is evident that for samples a starting p-type layer does not change the profile of the electrically active defects. It is typical for ion implantation in MCT. The profile depths are substantially more than R_p of implanted ions [4]. The

concentration at the maximum of the distribution curve is about 10^{18} cm^{-3} . For a sample of the original n-type subjected to irradiation in addition, post-annealing electric profile lies somewhat deeper, which corresponds to the data in ref. [5]. Thus, it can be argued that defects introduced by irradiation are being eliminated, while the implanted impurity is being activated during the annealing process. It should be noted that the parameters of the samples after etching of 1.5 microns of material have virtually returned to the value prior to irradiation.

CVC are shown in Figures 3-5. Up to a depth of 3 μm all CVC have an ohmic character. For samples 5 series diode current-voltage characteristic appears at a depth of 3 μm (Figures 3, 4), which corresponds to a depth profile of arsenic after implantation and post implantation annealing [5]. Therefore, the formation of a p-n junction can be attributed to the activation of arsenic in the annealing process in this case.

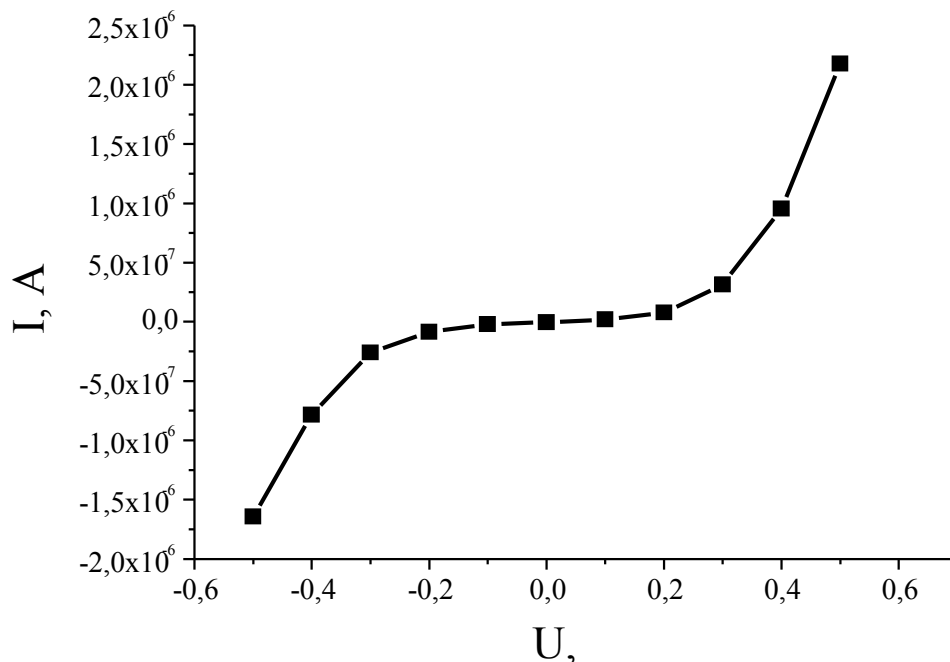


Figure 3. The current-voltage characteristic of the sample number 5 after 350 keV As ions implantation and post-annealing and etching of 3 μm .

It should be noted that the depth of the p-n junction does not depend on the energy of the implanted ions, while the electrical characteristics are different. This difference may be explained by the different concentration of activated arsenic in the region of the p-n junction.

For sample number 4 a diode type current-voltage characteristic is found only at a depth of 10 microns, which is far beyond the electrical profile and implanted arsenic profiles (Figure 2). Probably, the formation of the p-n junction is due to the deep diffusion of radiation-induced defects, the concentration of which cannot be detected by electrical measurements.

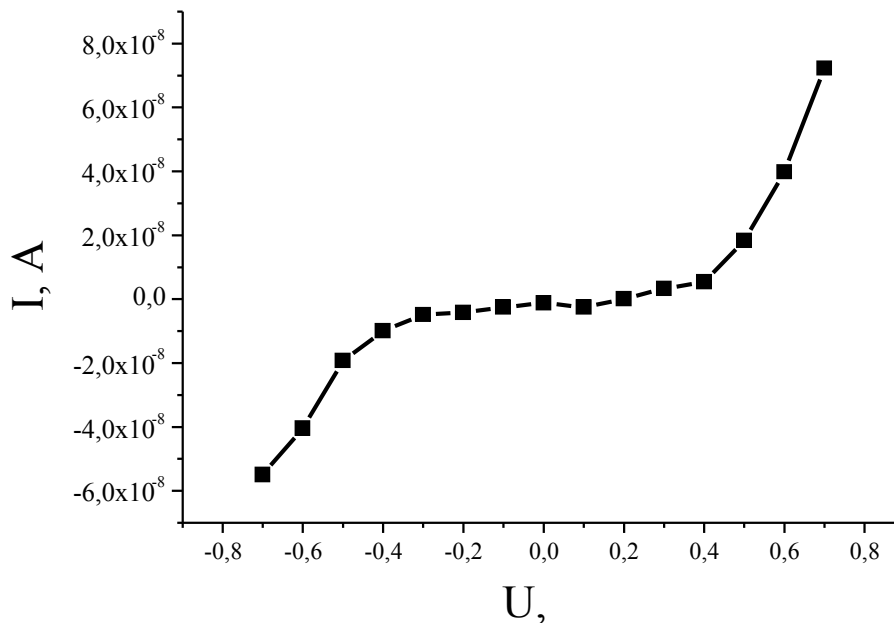


Figure 4. The current-voltage characteristic of the sample number 5 after 190 keV As ions implantation and post-annealing and etching of 3 μm .

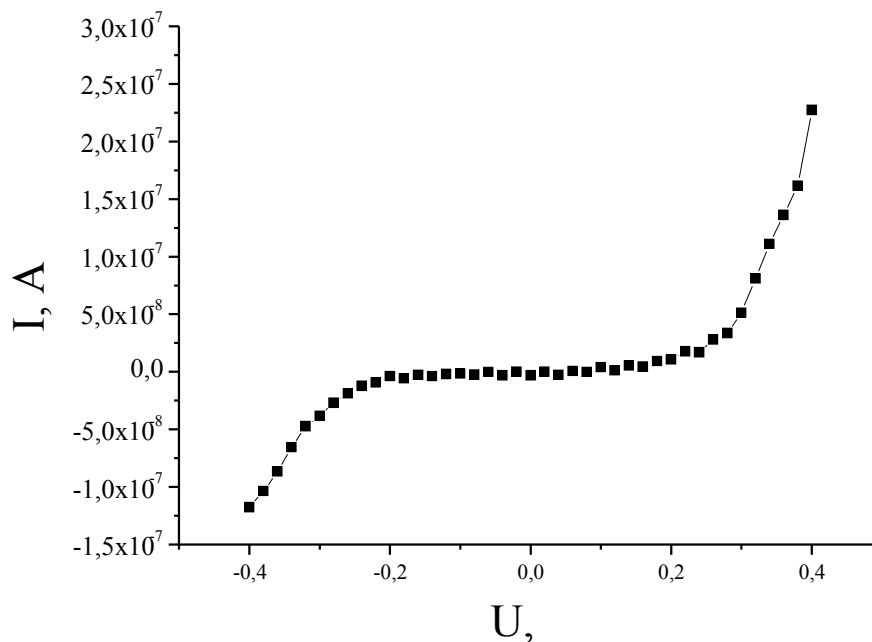


Figure 5. The current-voltage characteristic of the sample number 4 after 190 keV As ions implantation and etching of 10 μm .

4. Conclusion

Measurements of the electrical parameters showed the classic pattern similar to MCT samples after ion implantation. The influence of the presence of a variable-gap layer on the surface of the material and the substrate on the ion implantation results was shown.

It was noted that there is a decrease in the concentration of the layer at high doses, which can be explained by greater disorder of the implanted layer through the use of high-arsenic and heavy ions.

Significant differences in the p-n junctions depths for the obtained structures and in the measured profiles of distribution of electrically active defects are found. It is proposed to explain this distinction by the presence of the "tails" with low concentration of electrical defects and impurities.

References

- [1] Rogalski A 2011 *Infrared Detectors* (CRC Press, Boca Raton)
- [2] Mollard L., Destefanis G., Baier N., Rothman J., Ballet P., Zanatta J.P., Tchagaspian M., Papon A.M., Bourgeois G., Barnes J.P., Pautet C. 2009 *J. Electron. Mat.* **38**(8) 1805
- [3] Destefanis G.L. 1988 *J. Cryst. Growth.* **86** 700
- [4] Wang L., Zhang L.H. 2000 *J. Electron. Mat.* **29**(6) 873
- [5] Shin S.H., Arias J.M., Zandian M., Pasko J.G., Bubulac L.O., De Wames R.E. 1995 *J. Electron. Mat.* **24**(5) 615